# NEUTRINO INTERACTIONS WITH FLUKA*

G. Battistoni, P.R. Sala

INFN, Sezione di Milano, Via Celoria 16, 20133 Milan, Italy

M. Lantz

RIKEN Nishina Center for Accelerator-Based Science, Wako, Japan

A. Ferrari, G. Smirnov

CERN, 1211 Genève 23, Switzerland

*(Received July 17, 2009)*

A new neutrino interaction generator has been developed in FLUKA. The package, called NUNDIS (NeUtrino–Nucleon Deep Inelastic Scattering), is specifically built in order to be fully integrated with the hadronization and nuclear models of the FLUKA Monte Carlo code which were already successfully tested in hadronic interactions. This generator thus complements the already existing generator of quasi-elastic neutrino scattering. Here we describe the physics, sampling methods, and other specifics of NUNDIS, as well as the limitations of the code.

PACS numbers: 13.15.+g, 25.30.Pt, 21.60.Ka, 24.10.Lx

## 1. Introduction

The FLUKA Monte Carlo code is a general purpose simulation code for the interaction and transport of particles and nuclei in matter [1]. The generation of neutrino interactions is one of the development projects of the FLUKA Collaboration. The first step of such a project has been the introduction of a package for the Quasi-Elastic interactions, following the model of Ref. [2], with the idea of having a full integration with the nuclear model of FLUKA *i.e.* the PEANUT package. The performances of this model, with particular attention to the aspects concerning the nuclear effects, have been

* Presented at the 45th Winter School in Theoretical Physics "Neutrino Interactions: From Theory to Monte Carlo simulations", Lądek-Zdrój, Poland, February 2–11, 2009.

reported before [3–5]. Special models for solar $\nu$-interactions on argon were also introduced in the framework of the work for the ICARUS Collaboration [6]. In the same experimental context, the generation of Deep Inelastic neutrino interactions was addressed with FLUKA by means of the coupling to the external NUX generator [3,7]. Once again both initial and final state nuclear effects were managed by PEANUT (see [4,5]). The fundamental ansatz behind this choice is that the same nuclear models which give satisfactory results in hadronic interactions will be valid independently from the primary vertex. Therefore they should be valid also in neutrino interactions.

The experience with NUX was useful to produce results for the ICARUS Collaboration, however. we considered the idea of building a new dedicated DIS generator (and later a Resonance event generator) totally embedded in FLUKA from the partonic point of view. There are three main reasons for that:

(a) NUX hadronization is handled by PYTHIA [8], *i.e.* with another external package, independent from the hadronization package of FLUKA and therefore with additional and separate parameters. The consistency of models and the minimization of the number of parameters is instead a requisite of the FLUKA design.

(b) NUX does not contain a true description of resonance reactions. They are considered in average in the sampling of DIS events, according to the duality principle.

(c) NUX was neither publically distributed nor used outside the ICARUS Collaboration.

In this paper we briefly describe NUNDIS, the new Deep Inelastic Scattering event generator for neutrinos designed to be fully integrated in FLUKA, using the same hadronization routines as hadron–nucleon interactions and coupled to PEANUT as far as nuclear target environment is concerned.

## 2. Generalities on NUNDIS

The NUNDIS package has been designed to handle Neutral Current (NC) and Charged Current (CC) interactions for incident neutrinos and antineutrinos on protons and neutrons, on the basis of standard PDF sets (with extrapolation to $Q^2 = 0$), in the energy range from threshold to at least 10 TeV.

NUNDIS samples neutrino–nucleon Deep Inelastic Scattering reactions, returns to FLUKA a set of variables including the squared four-momentum transfer, $Q^2$. the mass squared of the hadronic system, $W^2$, the flavor of the parton that interacts with the neutrino. The code also determines if the interacting parton is a valence quark or a sea quark and the flavor of the outgoing interacting parton after the interaction. NUNDIS calculates the momentum and scattering angle of the outgoing lepton. In CC interactions the polarization of the outgoing charged lepton is also evaluated. Extrapolations are performed for $Q^2$ whenever this variable is beyond the range defined by the PDF-set.

## 3. Kinematics and constraints

The typical Feynman diagrams of the interactions simulated by NUNDIS are shown in Fig. 1 where the nature of incoming and outgoing lepton and of the intermediate vector boson are determined according to the sampling of CC or NC interactions.

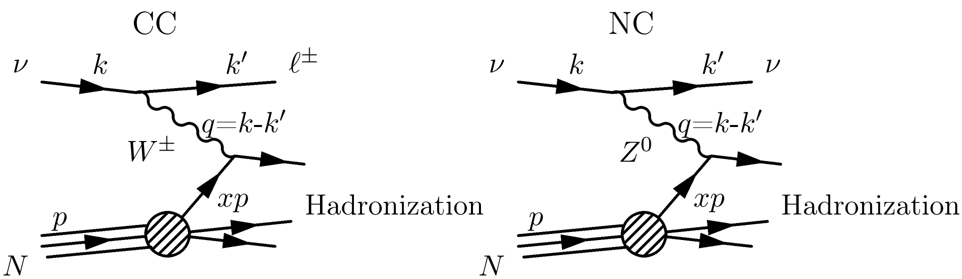


Fig. 1. Feynman diagrams of deep inelastic neutrino–nucleon scattering for Charged Current (left) and Neutral Current interaction (right). The letters represent kinematic variables: four momenta, momentum transfer and Bjorken-$x$.

The incident neutrino, $\nu_i$, where $i = e, \mu, \tau$, is assumed to be massless. Energy and momentum of the incident neutrino are set in FLUKA as properties of the primary particle. The target nucleon, $N$, with mass $M$, has in general a non-zero momentum in the laboratory frame (see Section 8). The reaction is then considered in the nucleon rest frame. Lorentz boosts to the nucleon rest frame are performed before entering NUNDIS. The final products are boosted back to the laboratory system.

The outgoing hadronic system, $X$, has invariant mass $W$, subject to the constraint

$$s > (W_{\rm min} + m_\ell)^2 \,, \tag{1}$$

where $m_\ell = 0$ in NC interactions. Therefore, $W$ is within the limits $W_{\rm min} \leq W \leq W_{\rm max}$, where

$$W_{\rm min} = M + m_\pi \,, \tag{2}$$

$$W_{\rm max} = \sqrt{s} - m_\ell \,. \tag{3}$$

The variable $Q^2$ is sampled within the limits $Q^2_{\rm min} \le Q^2 \le Q^2_{\rm max}$ with

$$Q^2_{\rm min} = 2E^*_\nu(E^*_\ell - |\bar{p}^*_\ell|) - m^2_\ell \,, \tag{4}$$

$$Q^2_{\rm max} = 2E^*_\nu(E^*_\ell + |\bar{p}^*_\ell|) - m^2_\ell = Q^2_{\rm min} + 4|\bar{p}^*_\nu||\bar{p}^*_\ell| \,, \tag{5}$$

where the outgoing lepton energy and momentum are set to the limit for single pion production:

$$E^*_\ell = \frac{s - (M + m_\pi)^2 + m^2_\ell}{2\sqrt{s}} \,, \tag{6}$$

$$|\bar{p}^*_\ell| = \sqrt{E^{*2}_\ell - m^2_\ell} = \sqrt{(E^*_\ell + m_\ell)(E^*_\ell - m_\ell)} \,. \tag{7}$$

The kinematical limits for Bjorken-$x$, the fraction of the nucleon momentum carried by the struck parton in the infinite momentum frame, are energy-dependent, and are taken from the derivation of Albright and Jarlskog [9] (with corrections of typographic errors given in Ref. [10]):

$$x_{\rm min} = \frac{m^2_\ell}{2M(E_\nu - m_\ell)} \,, \tag{8}$$

$$x_{\rm max} = 1 \,. \tag{9}$$

In addition, $x$ has to satisfy the following constraints which are $Q^2$-dependent:

$$x_{\rm min} = \frac{Q^2}{W^2_{\rm max} - M^2 + Q^2} \,, \tag{10}$$

$$x_{\rm max} = \frac{Q^2}{W^2_{\rm min} - M^2 + Q^2} \,, \tag{11}$$

so for a given sampled $Q^2$ the most strict limits are selected.

The kinematical limits for $y$ are taken from Refs [9, 10]:

$$a - b \le \; y \; \le a + b \,, \tag{12}$$

$$a = \frac{1 - m^2_\ell\left(\frac{1}{2ME_\nu x} + \frac{1}{2E^2_\nu}\right)}{2\left(1 + \frac{Mx}{2E_\nu}\right)} = \frac{E_\nu - \frac{m^2_\ell}{2}\left(\frac{1}{Mx} + \frac{1}{E_\nu}\right)}{2E_\nu + Mx} \,,$$

$$b = \frac{\sqrt{\left(1 - \frac{m^2_\ell}{2ME_\nu x}\right)^2 - \frac{m^2_\ell}{E^2_\nu}}}{2\left(1 + \frac{Mx}{2E_\nu}\right)}$$

$$= \frac{\sqrt{\left[\left(E_\nu - \frac{m^2_\ell}{2Mx}\right) + m_\ell\right]\left[\left(E_\nu - \frac{m^2_\ell}{2Mx}\right) - m_\ell\right]}}{2E_\nu + Mx} \,,$$

where Eq. (8) has to be fulfilled in order to avoid a negative root for part $b$. Expressions (8)–(12) are valid for CC and NC interactions, though for NC interactions the lower limit of $x$ is arbitrarily set to $10^{-15}$ in NUNDIS in order to work with the PDF-sets ($x$ has to be nonzero).

The outgoing lepton, $\ell^{\pm}$, where $\ell = e, \mu, \tau$, with mass $m_\ell$ will have scattering angle $\theta$ and four-vector $k'$:

$$k' = (E_\ell, \bar{p}_\ell) = (E_\ell, |\bar{p}_\ell| \sin\theta, 0, |\bar{p}_\ell| \cos\theta) \,, \tag{13}$$

$$E_\ell = E_\nu(1-y) \,, \tag{14}$$

$$|\bar{p}_\ell| = \sqrt{E_\ell^2 - m_\ell^2} = \sqrt{(E_\ell + m_\ell)(E_\ell - m_\ell)} \,, \tag{15}$$

$$\cos\theta = \frac{2E_\nu E_\ell - Q^2 - m_\ell^2}{2|\bar{p}_\nu||\bar{p}_\ell|} = \frac{2E_\nu E_\ell - Q^2 - m_\ell^2}{2E_\nu |\bar{p}_\ell|} \,. \tag{16}$$

For CC interactions the polarization of the outgoing lepton is of importance, especially for $\tau$ because its decay products have an angular distribution that depends on the polarization. For this purpose we follow the approach of Ref. [11].

## 4. The choice of PDF-set

Different PDF-sets have been considered [12–14]. Each set is defined within certain kinematical limits. If a variable is sampled or calculated outside of the defined limits of the selected PDF-set (with respect to $E$, $Q^2$ and $x$) a warning is given.

The thumb-rule is that it should be possible to cover the entire kinematical range of $Q^2$ and $x$ for neutrinos in the energy range 0–10 TeV. Table I gives the necessary kinematic ranges for 10 TeV neutrinos, followed by the stated limits for the PDF-sets under consideration. It also gives the upper

TABLE I

The required kinematical limits for 10 TeV neutrinos, followed by the given limits in the PDF-sets under consideration. For each set the first column gives the default limit and the second column gives the extended limit for which the PDF-sets have a stable behavior.

| | | GRV94 | | GRV98 | | BBS | |
|---|---|---|---|---|---|---|---|
| Variable | Required | Default | Tested | Default | Tested | Default | Tested |
| $E_{\min}$ (GeV) | — | 0.050 | | | | | |
| $E_{\max}$ (GeV) | $\geq 10^4$ | $70 \times 10^3$ | | | $10^5$ | | |
| $Q^2_{\min}$ (GeV$^2$) | $\leq 5.5 \times 10^{-12}$ | 0.4 | 0.4 | 0.8 | 0.8 | 2 | 0.8 |
| $Q^2_{\max}$ (GeV$^2$) | $\geq 1.9 \times 10^4$ | $10^6$ | $10^9$ | $10^6$ | $10^9$ | $10^4$ | $2 \times 10^4$ |
| $x_{\min}$ | $\leq 1.4 \times 10^{-11}$ | $10^{-5}$ | $10^{-30}$ | $10^{-9}$ | $10^{-30}$ | $10^{-4}$ | $10^{-30}$ |
| $x_{\max}$ | 1 | 0.99999 | 0.99999 | 1 | 1 | 1 | 1 |

and lower limits that have been tested and found to safely give a linear behavior. As seen all three PDF-sets under consideration fulfill all the requirements for 10 TeV neutrinos except for the lower $Q^2$-limit[1]. We have chosen GRV98 [13] as the default set.

Different approaches for extrapolation to $Q^2 = 0$ have been considered. The default method is based on the extrapolation of $F_i(Q^2, x)$ structure functions. These are described in Section 5.

The incident parton flavor determines the flavor of the outgoing parton, depending on whether it is NC or CC interaction. For example, Table II gives the relative probabilities for the transitions in neutrino CC interactions, and the nature of the resulting particles with minimum hadronic mass $W_{\min}$ to take into account. The relative probabilities are the square of the Cabibbo favored or suppressed angles. For *up*- and *down*-quarks this is also multiplied with the relative probability for the quark being valence- or sea-quark.

TABLE II

Relative probabilities for the transition of incident parton flavor to outgoing parton flavor, and minimum required hadronic mass, in CC $\nu$ and $\bar{\nu}$ interactions. The relative probabilities are the Cabibbo favored or suppressed transition fractions, and for *up*- and *down*-quarks there is also a factor for the valence- or sea-quark fraction.

| Process | | | Rel. prob. | $W_{\min}$ |
|---|---|---|---|---|
| $\nu + p$ | $\longrightarrow$ | $\ell^- + X$ | | |
| $\nu + (duu)$ | $\longrightarrow$ | $\ell^- + (uuu)$ | $\cos^2\theta_C \cdot v_d$ | $p + \pi^+$ |
| | $\longrightarrow$ | $\ell^- + (cuu)$ | $\sin^2\theta_C \cdot v_d$ | $\Lambda_c^+ + \pi^+$ |
| $\nu + d\bar{d}(duu)$ | $\longrightarrow$ | $\ell^- + u\bar{d}(duu)$ | $\cos^2\theta_C \cdot s_d$ | $p + \pi^+$ |
| | $\longrightarrow$ | $\ell^- + c\bar{d}(duu)$ | $\sin^2\theta_C \cdot s_d$ | $\Lambda_c^+ + \pi^+$ |
| $\nu + \bar{u}u(duu)$ | $\longrightarrow$ | $\ell^- + \bar{d}u(duu)$ | $\cos^2\theta_C$ | $p + \pi^+$ |
| | $\longrightarrow$ | $\ell^- + \bar{s}u(duu)$ | $\sin^2\theta_C$ | $p + K^+$ |
| $\nu + s\bar{s}(duu)$ | $\longrightarrow$ | $\ell^- + c\bar{s}(duu)$ | $\cos^2\theta_C$ | $\Lambda_c^+ + K^+$ |
| | $\longrightarrow$ | $\ell^- + u\bar{s}(duu)$ | $\sin^2\theta_C$ | $p + K^+$ |
| $\nu + \bar{c}c(duu)$ | $\longrightarrow$ | $\ell^- + \bar{s}c(duu)$ | $\cos^2\theta_C$ | $\Lambda_c^+ + K^+$ |
| | $\longrightarrow$ | $\ell^- + \bar{d}c(duu)$ | $\sin^2\theta_C$ | $\Lambda_c^+ + \pi^+$ |
| $\nu + n$ | $\longrightarrow$ | $\ell^- + X$ | | |
| $\nu + (ddu)$ | $\longrightarrow$ | $\ell^- + (udu)$ | $\cos^2\theta_C \cdot v_d$ | $p + \pi^0$ |
| | $\longrightarrow$ | $\ell^- + (cdu)$ | $\sin^2\theta_C \cdot v_d$ | $\Lambda_c^+ + \pi^0$ |
| $\nu + d\bar{d}(ddu)$ | $\longrightarrow$ | $\ell^- + u\bar{d}(ddu)$ | $\cos^2\theta_C \cdot s_d$ | $p + \pi^0$ |
| | $\longrightarrow$ | $\ell^- + c\bar{d}(ddu)$ | $\sin^2\theta_C \cdot s_d$ | $\Lambda_c^+ + \pi^0$ |

[1] For BBS the upper $Q^2$-limit can be pushed higher but then it yields peculiar $x$-behavior for *down*-quarks and gluons.

| | | | | |
|---|---|---|---|---|
| $\nu + \bar{u}u(ddu)$ | $\longrightarrow$ | $\ell^- + \bar{d}u(ddu)$ | $\cos^2\theta_{\rm C}$ | $p + \pi^0$ |
| | $\longrightarrow$ | $\ell^- + \bar{s}u(ddu)$ | $\sin^2\theta_{\rm C}$ | $n + K^+$ |
| $\nu + s\bar{s}(ddu)$ | $\longrightarrow$ | $\ell^- + c\bar{s}(ddu)$ | $\cos^2\theta_{\rm C}$ | $\Lambda_c^+ + K^0$ |
| | $\longrightarrow$ | $\ell^- + u\bar{s}(ddu)$ | $\sin^2\theta_{\rm C}$ | $n + K^+$ |
| $\nu + \bar{c}c(ddu)$ | $\longrightarrow$ | $\ell^- + \bar{s}c(ddu)$ | $\cos^2\theta_{\rm C}$ | $\Lambda_c^+ + K^0$ |
| | $\longrightarrow$ | $\ell^- + \bar{d}c(ddu)$ | $\sin^2\theta_{\rm C}$ | $\Lambda_c^+ + \pi^0$ |
| $\bar{\nu} + p$ | $\longrightarrow$ | $\ell^+ + X$ | | |
| $\bar{\nu} + (uud)$ | $\longrightarrow$ | $\ell^+ + (dud)$ | $\cos^2\theta_{\rm C} \cdot v_u$ | $n + \pi^0$ |
| | $\longrightarrow$ | $\ell^+ + (sud)$ | $\sin^2\theta_{\rm C} \cdot v_u$ | $\Lambda^0 + \pi^0$ |
| $\bar{\nu} + u\bar{u}(duu)$ | $\longrightarrow$ | $\ell^+ + d\bar{u}(duu)$ | $\cos^2\theta_{\rm C} \cdot s_u$ | $n + \pi^0$ |
| | $\longrightarrow$ | $\ell^+ + s\bar{u}(duu)$ | $\sin^2\theta_{\rm C} \cdot s_u$ | $\Lambda^0 + \pi^0$ |
| $\bar{\nu} + \bar{d}d(duu)$ | $\longrightarrow$ | $\ell^+ + \bar{u}d(duu)$ | $\cos^2\theta_{\rm C}$ | $n + \pi^0$ |
| | $\longrightarrow$ | $\ell^+ + \bar{c}d(duu)$ | $\sin^2\theta_{\rm C}$ | $n + \bar{D}^0$ |
| $\bar{\nu} + \bar{s}s(duu)$ | $\longrightarrow$ | $\ell^+ + \bar{c}s(duu)$ | $\cos^2\theta_{\rm C}$ | $\Lambda^0 + \bar{D}^0$ |
| | $\longrightarrow$ | $\ell^+ + \bar{u}s(duu)$ | $\sin^2\theta_{\rm C}$ | $\Lambda^0 + \pi^0$ |
| $\bar{\nu} + c\bar{c}(duu)$ | $\longrightarrow$ | $\ell^+ + s\bar{c}(duu)$ | $\cos^2\theta_{\rm C}$ | $\Lambda^0 + \bar{D}^0$ |
| | $\longrightarrow$ | $\ell^+ + d\bar{c}(duu)$ | $\sin^2\theta_{\rm C}$ | $n + \bar{D}^0$ |
| $\bar{\nu} + n$ | $\longrightarrow$ | $\ell^+ + X$ | | |
| $\bar{\nu} + (udd)$ | $\longrightarrow$ | $\ell^+ + (ddd)$ | $\cos^2\theta_{\rm C} \cdot v_u$ | $n + \pi^-$ |
| | $\longrightarrow$ | $\ell^+ + (sdd)$ | $\sin^2\theta_{\rm C} \cdot v_u$ | $\Lambda^0 + \pi^-$ |
| $\bar{\nu} + u\bar{u}(ddu)$ | $\longrightarrow$ | $\ell^+ + d\bar{u}(ddu)$ | $\cos^2\theta_{\rm C} \cdot s_u$ | $n + \pi^-$ |
| | $\longrightarrow$ | $\ell^+ + s\bar{u}(ddu)$ | $\sin^2\theta_{\rm C} \cdot s_u$ | $\Lambda^0 + \pi^-$ |
| $\bar{\nu} + \bar{d}d(ddu)$ | $\longrightarrow$ | $\ell^+ + \bar{u}d(ddu)$ | $\cos^2\theta_{\rm C}$ | $n + \pi^-$ |
| | $\longrightarrow$ | $\ell^+ + \bar{c}d(ddu)$ | $\sin^2\theta_{\rm C}$ | $n + D^-$ |
| $\bar{\nu} + \bar{s}s(ddu)$ | $\longrightarrow$ | $\ell^+ + \bar{c}s(ddu)$ | $\cos^2\theta_{\rm C}$ | $\Lambda^0 + D^-$ |
| | $\longrightarrow$ | $\ell^+ + \bar{u}s(ddu)$ | $\sin^2\theta_{\rm C}$ | $\Lambda^0 + \pi^-$ |
| $\bar{\nu} + c\bar{c}(ddu)$ | $\longrightarrow$ | $\ell^+ + s\bar{c}(ddu)$ | $\cos^2\theta_{\rm C}$ | $\Lambda^0 + D^-$ |
| | $\longrightarrow$ | $\ell^+ + d\bar{c}(ddu)$ | $\sin^2\theta_{\rm C}$ | $n + D^-$ |

The lower limit of $W^2$ has been set for single pion production according to Eq. (2). Now this limit may be increased depending on the parton transition. The actual value of $W^2_{\rm min}$ is set according to Table I (and similarly for NC interactions). Then the calculated $W^2$ has to be checked if it is above the lower limit. If not, then the event is rejected and a new attempt is made starting from the sampling of $Q^2$.

## 5. Structure functions

The calculation of structure functions is essential for the sampling of $Q^2$ and Bjorken-$x$. The structure functions follow the standard definition given by the Particle Data Group [15]. More specifically we use the definitions given in Ref. [16]. We follow the convention of isospin symmetry, so the flip of *up*- and *down*-quarks for neutrons has already been performed in the definition of the structure functions. For clarity we give the structure functions first with the real parton flavor, followed by the way they are given in the code when the isospin symmetry convention is used.

The considered CC structure functions are:

$$\begin{aligned}
F_2^{\nu p}\left(Q^2,x\right) &= 2x[d+\bar{u}+s+\bar{c}]\,, && (17)\\
xF_3^{\nu p}\left(Q^2,x\right) &= 2x[d-\bar{u}+s-\bar{c}]\,, && (18)\\
F_2^{\nu n}\left(Q^2,x]\right) &= 2x[u+\bar{d}+s+\bar{c}]\,, && (19)\\
xF_3^{\nu n}\left(Q^2,x\right) &= 2x[u-\bar{d}+s-\bar{c}]\,, && (20)\\
F_2^{\bar{\nu} p}\left(Q^2,x\right) &= 2x[u+\bar{d}+c+\bar{s}]\,, && (21)\\
xF_3^{\bar{\nu} p}\left(Q^2,x\right) &= 2x[u-\bar{d}+c-\bar{s}]\,, && (22)\\
F_2^{\bar{\nu} n}\left(Q^2,x\right) &= 2x[d+\bar{u}+c+\bar{s}]\,, && (23)\\
xF_3^{\bar{\nu} n}\left(Q^2,x\right) &= 2x[d-\bar{u}+c-\bar{s}]\,. && (24)
\end{aligned}$$

While the NC structure functions are given by:

$$F_2^{(\nu p,\bar{\nu}p)}\left(Q^2,x\right) = 2x\left[\left(g_{\rm L}^2+g_{\rm R}^2\right)[u+\bar{u}+c+\bar{c}]+\left(g_{\rm L}^{\prime 2}+g_{\rm R}^{\prime 2}\right)\left[d+\bar{d}+s+\bar{s}\right]\right]\,, \quad (25)$$

$$F_2^{(\nu n,\bar{\nu}n)}\left(Q^2,x\right) = 2x\left[\left(g_{\rm L}^2+g_{\rm R}^2\right)[u+\bar{u}+c+\bar{c}]+\left(g_{\rm L}^{\prime 2}+g_{\rm R}^{\prime 2}\right)\left[d+\bar{d}+s+\bar{s}\right]\right]\,, \quad (26)$$

$$F_3^{(\nu p,\bar{\nu}p)}\left(Q^2,x\right) = 2x\left[\left(g_{\rm L}^2-g_{\rm R}^2\right)[u-\bar{u}+c-\bar{c}]+\left(g_{\rm L}^{\prime 2}-g_{\rm R}^{\prime 2}\right)\left[d-\bar{d}+s-\bar{s}\right]\right]\,, \quad (27)$$

$$F_3^{(\nu n,\bar{\nu}n)}\left(Q^2,x\right) = 2x\left[\left(g_{\rm L}^2-g_{\rm R}^2\right)[u-\bar{u}+c-\bar{c}]+\left(g_{\rm L}^{\prime 2}-g_{\rm R}^{\prime 2}\right)\left[d-\bar{d}+s-\bar{s}\right]\right]\,, \quad (28)$$

where

$$\begin{aligned}
g_{\rm L} &= \tfrac{1}{2}-\tfrac{2}{3}\sin^2\theta_{\rm W}\,,\\
g_{\rm R} &= -\tfrac{2}{3}\sin^2\theta_{\rm W}\,,\\
g'_{\rm L} &= -\tfrac{1}{2}+\tfrac{1}{3}\sin^2\theta_{\rm W}\,,\\
g'_{\rm R} &= \tfrac{1}{3}\sin^2\theta_{\rm W}\,, && (29)
\end{aligned}$$

and $\theta_{\rm W}$ is the Weinberg angle with $\sin^2\theta_{\rm W} = 0.23122$, which corresponds to the value determined from all available data [17] in the framework of the modified minimal subtraction ($\overline{\rm MS}$) scheme.

At the moment, $F_1(Q^2,x)$ is defined through the Callan–Gross relation [18]: $F_1 = F_2/2x$. In the next release this will be replaced by introducing the ratio of the cross-section for scattering from longitudinally to transversely polarized bosons.

$F_4$ and $F_5$ follow the Albright–Jarlskog relations [9], $F_4 = 0, F_5 = \frac{F_2}{x}$. These relations are valid in leading order and will do well for the time being.

As far as the extrapolation to $Q^2 = 0$ is concerned, the default method is based on the extrapolation of $F_i(Q^2,x)$ functions. A simple approach inspired by the two-phase model is at the moment employed in NUNDIS. For $Q^2 < Q_0^2$ we rescale the structure functions according to

$$F_i(Q^2,x) = \frac{2Q^2}{Q_0^2 + Q^2} F_i(Q_0^2,x)\,. \tag{30}$$

## 6. Cross-sections

The integration of differential cross-sections is used for the sampling of $Q^2$ and $x$, and to generate the tables of cross-section data.

The double differential cross-sections are calculated and defined according to Paschos and Yu [16]:

$$\frac{d^2\sigma}{dxdQ^2} = \frac{d^2\sigma}{dxdy}\frac{dy}{dQ^2} = \frac{d^2\sigma}{dxdy}\frac{1}{2ME_\nu x}\,, \tag{31}$$

$$\frac{d^2\sigma}{dxdy} = \frac{G_\mathrm{F}^2 M E_\nu}{\pi\left(1+Q^2/M_{W/Z}^2\right)^2}\sum_{i=1}^{5} A_i(x,y,E_\nu)F_i\left(Q^2,x\right)\,, \tag{32}$$

where $G_\mathrm{F}$ is the Fermi constant, $M_{W/Z}$ is the vector boson mass ($M_W$ for CC and $M_Z$ for NC interactions), and the coefficients $A_i(x,y,E_\nu)$ are

$$\begin{aligned}
A_1 &= y\left(xy + \frac{m_\ell^2}{2ME_\nu}\right)\,,\\
A_2 &= 1 - y\left(1+\frac{Mx}{2E_\nu}\right) - \frac{m_\ell^2}{4E_\nu^2}\,,\\
&= \left(1+\frac{m_\ell}{2E_\nu}\right)\left(1-\frac{m_\ell}{2E_\nu}\right) - y\left(1+\frac{Mx}{2E_\nu}\right)\,,
\end{aligned}$$

$$\begin{aligned} A_3 &= \pm y\left[x\left(1-\frac{y}{2}\right)-\frac{m_\ell^2}{4ME_\nu}\right], \\ A_4 &= \frac{m_\ell^2}{2ME_\nu}\left(y+\frac{m_\ell^2}{2ME_\nu x}\right), \\ A_5 &= -\frac{m_\ell^2}{ME_\nu}\,. \end{aligned} \tag{33}$$

The minus sign for $A_3$ is used for anti-neutrinos.

The double differential cross-section for the outgoing lepton is calculated according to the relation

$$\frac{d\sigma}{dE_\ell d\cos\theta}=\frac{G_{\mathrm{F}}^2}{2\pi}\frac{p_\ell}{M}\left(\frac{M_W^2}{M_W^2+Q^2}\right)^2 F\,, \tag{34}$$

where $F$ is given by:

$$\begin{aligned} F &= \left(2\,W_1+\frac{m_\ell^2}{M^2}W_4\right)(E_\ell-|\bar{p}_\ell|\cos\theta)+W_2(E_\ell+|\bar{p}_\ell|\cos\theta) \\ &\quad \pm\frac{W_3}{M}\left(E_\nu E_\ell+|\bar{p}_\ell^2|-(E_\nu+E_\ell)|\bar{p}_\ell|\cos\theta\right)-\frac{m_\ell^2}{M}W_5\,, \\ P &= 2\sqrt{s_x^2+s_y^2+s_z^2}\,, \\ W_1 &= F_1\left(Q^2,x\right)\,, \\ W_{i=2\ldots5} &= \frac{M^2}{p\cdot q}F_{i=2\ldots5}\left(Q^2,x\right)=\frac{2M^2x}{Q^2}F_{i=2\ldots5}\left(Q^2,x\right)\,. \end{aligned} \tag{35}$$

The total cross-sections tables are calculated by means of numerical integration of double differential cross-sections.

## 7. Hadronization

The output from the sampling of DIS events, at parton level, is passed to the hadronization package of FLUKA which is based on the BAMJET package [19]. The principle is the following. If, for instance, the neutrino interacts with a valence quark of the nucleon, the constituent partons are split into a diquark and the quark resulting in the final state. An hadronic chain (string) carrying no net color is stretched between the quark and the diquark. The hadronization model takes care of transforming the chain into a sequence of physical particles, stable ones or resonances. The hadronization properties are the same as in hadronic interactions on the basis of the assumption of universality. More than a single chain has to be hadronized whenever quark–antiquark pairs are excited from the sea. This is necessary when the neutrino interaction occurs on a sea quark.

## 8. The treatment of nuclear effects by PEANUT

The nuclear environment in FLUKA is managed by the PEANUT package. All properties concerning the initial status of the target nucleon in the nucleus and all final state reinteractions are taken into account at this stage.

A standard position dependent Fermi momentum distribution is implemented in PEANUT up to a local Fermi momentum $k_{\mathrm{F}}(r)$ depending on the nuclear density $\rho^{p,n}(r)$ at a given point in the nucleus and separately evaluated for protons and neutrons. Proton and neutron densities are generally different, according again to shell model ones for $A < 16$, and to the droplet model [20] for heavier nuclei.

Fermi momentum is smeared according to the uncertainty principle assuming a position uncertainty $= \sqrt{2}$ fm. The potential depth felt by nucleons at any radius $r$ is given by the Fermi energy plus the relevant binding energy. Binding energies are obtained from mass tables, depending on particle type and on the actual composite nucleus, which may differ from the initial one in case of multiple particle emission. Fermi motion is taken into account, both to compute the interaction cross-section, and to produce the final state particles.

As far as reinteractions are concerned, at present PEANUT handles the interaction processes of nucleons, pions, kaons, and $\gamma$ rays from a few GeV down to reaction threshold (or 20 MeV for neutrons). The reaction mechanism is modeled in PEANUT by an explicit Generalized INtranuclear Cascade (GINC) smoothly joined to statistical (exciton) preequilibrium emission [21, 22]. At the end of the GINC and exciton chain, the evaporation of nucleons and light fragments ($\alpha$, $d$, $^3$H, $^3$He) is performed, following the Weisskopf [23] treatment. Competition of fission with evaporation has been implemented, again within a statistical approach. For light nuclei, the so called Fermi Break-up model [24, 25] is used instead. The excited nucleus is supposed to disassemble just in one step into two or more fragments, with branching given by plain phase space considerations, corrected for Coulomb barriers when applicable. The excitation energy still remaining after (multiple) evaporation is dissipated via emission of $\gamma$ rays [26]. The GINC proceeds through hadron multiple collisions in a cold Fermi gas. The hadron–nucleon cross-sections used in the calculations are the free ones modified by Pauli blocking, except for pions and negative kaons that deserve a special treatment. Secondaries are treated exactly like primary particles, with the only difference that they start their trajectory already inside the nucleus. Primary and secondary particles are transported according to their nuclear mean field and to the Coulomb potential. All particles are transported along classical trajectories, nevertheless a few relevant quantum effects are included. In both stages, INC and exciton, the nucleus is modeled as a sphere with density given by a symmetrized Woods–Saxon [27] shape for $A > 16$ and by a harmonic oscillator shell model for light isotopes (see [28]).

For pions, a nuclear potential has been calculated starting from the standard pion–nucleus optical potential [29]. Two-and three-nucleon absorption processes are considered. Above the pion production threshold, the inelastic interactions are handled by a resonance model. Other pion–nucleon interactions proceed through the non-resonant channel and the $p$-wave channel with the formation of a $\Delta$ resonance. In nuclear matter, the $\Delta$ can either decay, resulting in elastic scattering or charge exchange, or interact with other nucleons, resulting in pion absorption. We make use of the approach outlined in [30], where the partial widths for quasi-elastic scattering, two body and three body absorption are considered. Isospin relations are extensively applied both to derive the pion–nucleon cross-sections in any given charge configuration from the three experimentally known, and to weight the different interaction and decay channels of the $\Delta$ resonance [31, 32]. Angular distributions of reaction products are sampled according to experimental data both for pion scattering (from free pion–nucleon) and pion absorption (from absorption on $^3$He and deuterium).

The naive use of free hadron–nucleon cross-sections would lead to hadron mean free paths in nuclei by far too short with respect to reality. Indeed there are many effects that influence the in-medium cross-sections, and some of them are accounted for in FLUKA. The most important ones are Pauli blocking, nucleon antisymmetrization effects, nucleon–nucleon hard-core correlations, formation zone and coherence length.

## 9. Resonance scattering

In addition to NUNDIS, a new package called NUNRES in now under development with the purpose to generate (anti)neutrino–nucleon resonance interactions. It is built on the basis of the Rein–Sehgal formulation [33]. It considers only $\Delta$ production. No non-resonant background term is considered, assuming that the non-resonance contribution comes from NUNDIS. For the moment, the transition from resonance to Deep Inelastic Scattering is performed imposing a linear decrease of both $\sigma$ as a function of $W$.

## 10. Conclusions

The NUNDIS and NUNRES codes are presently distributed as a beta-version release in the standard version FLUKA 2008. There, by means of the standard FLUKA input commands, neutrino primaries can be simulated forcing the interaction at a given location. Users have to weight results for the proper cross-sections which are distributed in a separate file. As an example, in Fig. 2 we show the CC cross-sections per nucleon for $\nu_\mu$ and $\bar{\nu}_\mu$ on an isoscalar target. To give an illustration of the results achievable with the code described here, in Fig. 3 we show the momentum distribution of

$\pi^+$ in $\nu_\mu$+$^{16}$O CC interactions at 1 GeV, where the $\mu^- + \pi^+ + X$ topology is selected in the final state. Due to nuclear effects both DIS and resonance scattering contribute to the selected channel. The figure shows how the distribution is affected by the reinteractions in the nucleus. Under these conditions about 73% of $\pi^+$ survive escaping nuclear absorption.

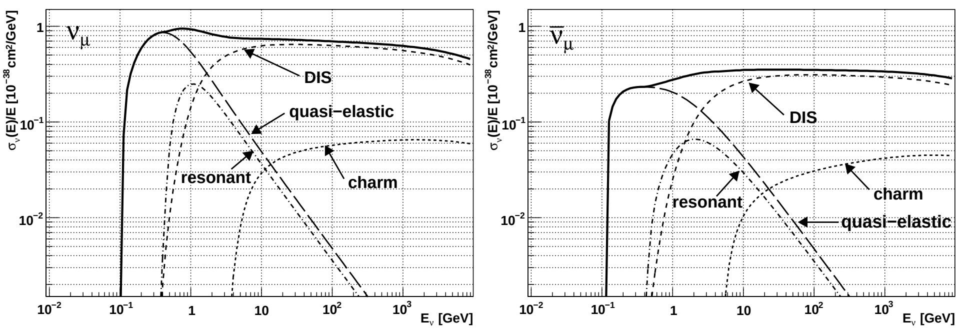


Fig. 2. CC cross-section ($\sigma(E)/E$) as a function of energy for $\nu_\mu$ (left) and $\bar{\nu}_\mu$ (right) as calculated from the NUNDIS and NUNRES packages of FLUKA. The thick solid line represents the total cross-section, but the different contributions are also displayed. The charm production is plotted separately from the DIS contribution.

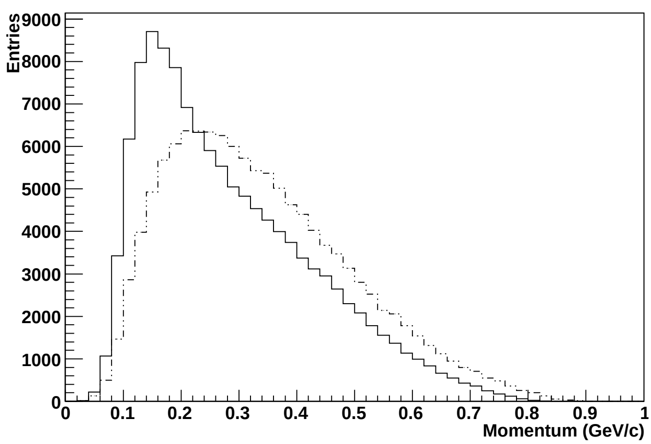


Fig. 3. Distribution of $\pi^+$ momentum in $\nu_\mu$+$^{16}$O CC interactions, where the $\mu^- + \pi^+ + X$ topology is selected in the final state. The continuous line histogram represents the distribution after nuclear reinteractions, while the dot-dashed line is relative to the distribution before final state interactions.

The NUNDIS and NUNRES packages represent a significant improvement in the FLUKA development and allow the treatment of neutrino interactions consistently with the rest of the FLUKA models. The code is still under development and several improvements are now planned. For example, target mass corrections of Bjorken-$x$ according to the Nachtmann variable [34] or suggestions by Bodek [35] have not yet been implemented. So far only some initial tests have been made. In the meantime, benchmarking with data from neutrino experiments at accelerators is in progress.

This work has been carried out in the framework of the FLUKA Collaboration. One of us (G.B.) wishes to thank M. Antonello and V. Caracciolo for the interest and the assistance given during the 45th Karpacz Winter School.

## REFERENCES

[1] A. Ferrari, P.R. Sala, A. Fassò, J. Ranft, CERN-2005-010, INFN/TC_05/11 (2005); G. Battistoni, S. Muraro, P.R. Sala, F. Cerutti, A. Ferrari, S. Roesler, A. Fassò, J. Ranft, Proc. of the Hadronic Shower Simulation Workshop 2006, Fermilab 6–8 September 2006, M. Albrow, R. Raja eds., *AIP Conf. Proc.* **896**, 31 (2007).

[2] C.H. Llewellyn-Smith, *Phys. Rep.* **3**, 261 (1972).

[3] G. Battistoni, A. Ferrari, A. Rubbia, P.R. Sala, Proceedings of the "Second International Workshop on Neutrino-Nucleus Interactions in the few-GeV Region", NUINT02, December 2002, University of California, Irvine, USA.

[4] G. Battistoni, P.R. Sala, A. Ferrari, Proc. of the 20th Max Born Symposium: Nuclear Effects in Neutrino Interactions, Wrocław, Poland, 7–10 Decebmer 2005, *Acta Phys. Pol. B* **37**, 2361 (2006).

[5] G. Battistoni, P.R. Sala, M. Lantz, A. Ferrari, G. Smirnov, Proc. of the 11th International Conference on Nuclear Reaction Mechanisms, Varenna, Italy, 12–16 June 2006, pp. 497–506.

[6] S. Amerio *et al.* [ICARUS Collaboration], *Nucl. Instrum. Methods* **527**, 329 (2004).

[7] A. Rubbia, 1st Workshop on Neutrino–Nucleus Interactions in the Few GeV Region (NuInt01), Tsukuba, Japan, 13–16 December 2001.

[8] T. Sjöstrand *et al.*, *Comput. Phys. Commun.* **135**, 238 (2001) `[hep-ph/0010017]`.

[9] C.H. Albright, C. Jarlskog, *Nucl. Phys.* **B84**, 467 (1975).

[10] S. Kretzer, M.H. Reno, *Phys. Rev.* **D66**, 113007 (2002).

[11] K. Hagiwara, K. Mawatari, H. Yokoya, *Nucl. Phys.* **B668**, 364 (2003), Erratum *Nucl. Phys.* **B701**, 405 (2004) `[hep-ph/0305324]`.

[12] M. Glück, E. Reya, A. Vogt, *Z. Phys.* **C67**, 433 (1995); `http://durpdg.dur.ac.uk/`

[13] M. Glück, E. Reya, A. Vogt, *Eur. Phys. J.* **C5**, 461 (1998) `[hep-ph/9806404]`; `http://durpdg.dur.ac.uk/`

[14] C. Bourrely, J. Soffer, F. Buccella, *Eur. J. Phys.* **C23**, 487 (2002) `[hep-ph/0109160]`; `http://www.cpt.univ-mrs.fr/ bourrely/research/bbs-dir/bbs.html`

[15] S. Eidelman *et al.* [Particle Data Group], *Phys. Lett.* **B592**, 1 (2004).

[16] E.A. Paschos, J.Y. Yu, *Phys. Rev.* **D65**, 033002 (2002).

[17] A.B. Balantekin, Editor-in-Chief, [Particle Data Group], *J. Phys. G: Nucl. Part. Phys.* **33**, 120 (2006).

[18] C.G. Callan, D.J. Gross, *Phys. Rev. Lett.* **22**, 156 (1969).

[19] S. Ritter, *Comput. Phys. Commun.* **31**, 393 (1984); J. Ranft, S. Ritter, *Acta Phys. Pol. B* **11**, 259 (1980).

[20] W.D. Myers, *Nucl. Phys.* **A204**, 465 (1973); W.D. Myers, *Droplet Model of Atomic Nuclei*, IFI/Plenum Data Company, New York 1977.

[21] E. Gadioli, P.E. Hodgson, *Pre-Equilibrium Nuclear Reactions*, Clarendon Press, Oxford 1992.

[22] J.J. Griffin, *Phys. Rev. Lett.* **17**, 438 (1966).

[23] V.F. Weisskopf, *Phys. Rev.* **52**, 295 (1937).

[24] E. Fermi, *Prog. Theor. Phys.* **5**, 1570 (1950).

[25] M. Epherre, E. Gradsztajn, *J. Phys.* **18**, 48 (1967).

[26] A. Ferrari, P.R. Sala, J. Ranft, S. Roesler, *Z. Phys.* **C71**, 75 (1996).

[27] M.E. Grypeos, G.A. Lalazissis, S.E. Massen, C.P. Panos, *J. Phys. G* **17**, 1093 (1991).

[28] L.R.B. Elton, *Nuclear Sizes*, Oxford University Press, Oxford 1961.

[29] T. Ericson, W. Weise, *Pions and Nuclei*, Clarendon Press, Oxford 1988.

[30] E. Oset, L.L. Salcedo, *Nucl. Phys.* **A468**, 631 (1987).

[31] J.N. Ginocchio, *Phys. Rev.* **C17**, 195 (1978).

[32] M.J. Vicente-Vacas, E. Oset, *Nucl. Phys.* **A568**, 855 (1994).

[33] D. Rein, L. Sehgal, *Ann. Phys.* **133**, 79 (1981).

[34] O. Nachtmann, *Nucl. Phys.* **B63**, 237 (1973).

[35] A. Bodek, U.K. Yang, *Nucl. Phys.* **B112**, 70 (2002).